

SYNCHROTRON AND COMPTON SPECTRA FROM A STEADY-STATE ELECTRON DISTRIBUTION

Y. REPHAELI¹

School of Physics and Astronomy, Tel Aviv University, Tel Aviv, 69978, Israel

AND

M. PERSIC²

INAF/Osservatorio Astronomico di Trieste and INFN-Trieste, via G.B. Tiepolo 11, I-34143 Trieste, Italy

Draft version April 16, 2021

ABSTRACT

Energy densities of relativistic electrons and protons in extended galactic and intracluster regions are commonly determined from spectral radio and (rarely) γ -ray measurements. The time-independent particle spectral density distributions are commonly assumed to have a power-law (PL) form over the relevant energy range. A theoretical relation between energy densities of electrons and protons is usually adopted, and energy equipartition is invoked to determine the mean magnetic field strength in the emitting region. We show that for typical conditions, in both star-forming and starburst galaxies, these estimates need to be scaled down substantially due to significant energy losses that (effectively) flatten the electron spectral density distribution, resulting in a much lower energy density than deduced when the distribution is assumed to have a PL form. The steady-state electron distribution in the nuclear regions of starburst galaxies is calculated by accounting for Coulomb, bremsstrahlung, Compton, and synchrotron losses; the corresponding emission spectra of the latter two processes are calculated and compared to the respective PL spectra. We also determine the proton steady-state distribution by taking into account Coulomb and π production losses, and briefly discuss implications of our steady-state particle spectra for estimates of proton energy densities and magnetic fields.

Subject headings: galaxies: spiral — galaxies: starburst; radiation mechanisms: non-thermal

1. INTRODUCTION

Nonthermal phenomena in galaxies and galaxy clusters are important for a more complete understanding of these systems, and for knowledge of the origin of relativistic particles and magnetic fields. Current and future measurement capabilities necessitate fairly detailed modeling of these quantities, and inclusion of the impact of interactions of relativistic particles in neutral and ionized magnetized media.

Measurements of radiative yields of relativistic electrons and protons across a wide spectral range provide the observational basis for determining their spectral density distributions (e.g., Schlickeiser 2002). Basic properties of these particles and their broad energy ranges are determined from measurements of radio, X-ray, and γ -ray emission from primary electrons and secondary electrons and positrons (produced in π^\pm decay) in synchrotron, bremsstrahlung, and Compton processes, as well as γ -ray emission from protons via π^0 decay. These spectral bands do not fully cover the particle very broad energy ranges, particularly at low energies. Consequently, there is an appreciable degree of indeterminacy in quantitative estimations of integrated quantities, most important of which are particle energy densities. Due to the approximate decreasing (with energy) PL form of the spectral density, the generally unknown value of the low energy cutoff introduces substantial uncertainty in both proton and electron energy densities. Yet, as we discuss in this paper, the implications of this uncertainty are quite significant.

Relativistic particles are one of the consequences of the formation and evolution of high-mass stars, so phenomena related to these particles are of interest in all star-forming galaxies. Reliable estimates of particle energy densities are very much needed for a quantitative evaluation of acceleration models and comparison with other measures of stellar evolutionary processes that give rise to high-energy phenomena, such as SN explosions, compact remnants of core collapse, and SN shocks, all of which are largely gauged by formation rates of high-mass stars (Torres et al. 2012, Persic & Rephaeli 2010).

For the purpose of assessing the significance of realistic estimation of their particle energy densities, galaxies in which high-energy phenomena are dominated by stellar activity are of particular interest. Among these, well-observed nearby galaxies are especially suited, such as the two nearby starburst (SB) galaxies M82 and NGC253, for which the gas properties in the nuclear SB region are well determined and their radio emission well mapped. Moreover, γ -ray emission from these galaxies has been detected by the *Fermi* Large Area Telescope at GeV energies (Ackermann et al. 2012), and at TeV energies by the Cherenkov arrays VERITAS and H.E.S.S (Acciari et al. 2009, Acero et al. 2009), at flux levels that are in agreement with theoretical predictions (Domingo-Santamaria & Torres 2005, Persic, Rephaeli, & Arieli 2008, de Cea et al. 2009, Rephaeli et al. 2010).

In this paper we assess the reliability of estimation of electron energy densities from measurements of synchrotron

yoelr@wise.tau.ac.il

¹ Center for Astrophysics and Space Sciences, University of California, San Diego, La Jolla, CA 92093-0424

² INFN-Trieste, via A. Valerio 2, I-34127 Trieste, Italy

radio emission, quantifying the significant over-estimation of particle energy densities in SBGs due to the common assumption of a PL form for the spectral density of the emitting electrons. In Section 2 we show that when all relevant electron energy losses are accounted for, the electron spectral density can obviously deviate significantly from a PL form, as had been quantitatively demonstrated long ago (e.g. Rephaeli 1979, Pohl 1993). This necessitates re-calculation of the synchrotron and Compton emissivities (Section 3). As we demonstrate in the latter section, normalization of the electron spectrum by comparison with radio measurements has significant consequences also for the predicted Compton X-ray and γ -ray spectra. The revised electron spectra yield significantly different estimates of the electron energy density than those obtained when the standard formula is used, as shown specifically (Section 4) for conditions in SB nuclei. We briefly discuss our results in Section 5.

2. STEADY-STATE ELECTRON DISTRIBUTION

It is commonly assumed that steady-state energetic particle (mostly electrons, protons, and helium nuclei) distributions can be well approximated by a PL form for a range of values $[\gamma_1, \gamma_2]$ of the Lorentz factor, γ ; for electrons, the spectral density is

$$N_{pl}(\gamma) = N_1 \gamma^{-q_{pl}}, \quad (1)$$

where N_1 is a normalization constant and q_{pl} is the spectral index. Since this commonly used form has no temporal dependence, it is implicitly *assumed* to be a steady-state distribution. This is the form used in the derivation of the standard formulae for electron synchrotron, bremsstrahlung, and Compton spectra. While this approximate single-index PL form may be sufficiently accurate for some purposes, it could be very inadequate when the relevant electron energy loss processes have different energy dependence.

In a SB nuclear (SBN) region intense star formation yields a high SN rate and consequently efficient particle acceleration. A galactic dynamical process, the SB phase is long, $O(10^8)$ year, and since energetic electrons and protons sustain significant energy losses in the relatively small gas-rich, magnetically and radiatively intense SBN source region, steady-state is expected. The theoretically predicted single index PL spectral density in the acceleration region evolves to become a curved steady-state profile as a result of energy loss processes. To determine the steady-state electron spectral density, we assume that the *initial* spectrum of primary accelerated electrons is a PL in momentum. Since we are mostly interested in the radiative yields of relativistic electrons with $\gamma \gg 1$, we express the single-index spectrum in terms of γ , and write for the injection rate per unit volume

$$\left(\frac{dN}{dt} \right)_i = k_i \gamma^{-q_i}, \quad (2)$$

where k_i is a normalization constant. When an exact description of the electron spectrum is needed (also) at low energies, $\gamma \sim 1$, the exact relation between energy and momentum has to be used, for which the γ dependence of the injection spectrum is $\gamma(\gamma^2 - 1)^{-(q_i+1)/2}$. Whereas the dependence of the electron density on γ_1 can be appreciable (as discussed below), and since typically $\gamma_2 > 10^6$, the exact value of this upper cutoff is of little significance for relevant values of q_i .

Energetic particle propagation out of their source region and throughout interstellar (IS) space is typically described as a combination of convection and diffusion. We assume that in the relatively small SBN region spatial density gradients are not significant, so that the particle density is roughly uniform. While particle escape out of the SBN is essentially a catastrophic loss that would generally be included as a sink term in the kinetic equation describing the spectral distribution, when this term is energy independent its overall impact essentially amounts to an overall constant factor in the expression for the (steady state) spectral density. Since in our treatment here the overall normalization of the electron density is set by the measured level of radio emission, this escape term does not have to be explicitly included in the equation for the steady state distribution. For our purposes here we therefore focus only on the spectral dependence of the steady-state electron density, $N(\gamma)$, which is determined by the energy dependence of the total energy loss rate, $-d\gamma/dt = b(\gamma)$. In this case the electron steady-state spectral density is determined by solving the simple kinetic equation

$$-\frac{d[b(\gamma)N(\gamma)]}{d\gamma} = k_i \gamma^{-q_i}. \quad (3)$$

The relevant energy loss processes in a magnetized (H-He) gas permeated by intense (IR) radiation field are ionization, electronic excitation (or Coulomb), bremsstrahlung, and synchrotron-Compton. The corresponding energy loss rates for these well-known processes are $b_0(\gamma)$, $b_1(\gamma)$, and $b_2(\gamma)$, respectively. In a medium which consists of ionized, neutral, and molecular gas with densities n_i , n_H , and n_{H_2} , respectively, the lower order energy loss of (a charged energetic particle) is by exciting plasma oscillations and by ionization. The expressions for the exact loss rate for electron energies down to the sub-relativistic regime were calculated by Gould (1972, 1975; see also Schlickeiser 2002); these yield the approximate total rate

$$b_0(\gamma) \simeq \frac{1.1 \times 10^{-12}}{\beta} \left[n_i \left(1.0 - \frac{\ln n_i}{74.6} \right) + 0.4(n_H + 2n_{H_2}) \right] s^{-1}, \quad (4)$$

where $\beta = (1 - \gamma^{-2})^{-1/2}$. In the strong shielding limit, an approximate expression for the closely related bremsstrahlung

loss rate is (Gould 1975)

$$b_1(\gamma) \simeq 1.8 \times 10^{-16} \gamma [n_i + 4.5(n_H + 2n_{H2})] s^{-1}. \quad (5)$$

The synchrotron-Compton loss rate of an electron in a magnetic field B and in a radiation field with energy density ρ_r is (e.g., Blumenthal & Gould 1970)

$$b_2(\gamma) \simeq 1.3 \times 10^{-9} \gamma^2 (B^2 + 8\pi\rho_r) s^{-1}. \quad (6)$$

We note that the range of electron energies relevant for our discussion does not extend to energies beyond the validity of the Thomson limit, i.e., the incident photon energy, ϵ_0 , in the electron frame, $\gamma\epsilon_0$, satisfies the inequality $\gamma\epsilon_0 \ll mc^2$ for all values of $\epsilon_0 < 0.01$ eV and $\gamma < 10^6$ of interest to us here. Obviously, the full Klein-Nishina cross section has to be used at much higher energies (e.g., Schlickeiser & Ruppel 2010). Aside from the weak (logarithmic) γ dependence in the expressions for b_0 and b_1 , the value of the subscript in each of the three loss rates corresponds to the power of its γ dependence, with the relative magnitude of each term determined by the gas densities, B , and the radiation field. At low energies the Coulomb rate dominates, whereas at high energies synchrotron-Compton losses dominate. The steady-state spectral electron density is then

$$N(\gamma) = \frac{k_i \gamma^{-(q_i-1)}}{b(\gamma)(q_i-1)}. \quad (7)$$

Clearly, the different energy dependence of the loss processes results in a curved steady-state spectral density, with the value of the effective PL index changing from $q_i - 1$ at energies for which Coulomb losses begin to dominate over the combined losses by bremsstrahlung and synchrotron-Compton, at energies well below

$$\gamma \leq 3.0 \times 10^3 \left(\frac{n_i}{100 \text{ cm}^{-3}} \right)^{1/2} \left(\frac{B}{100 \mu\text{G}} \right)^{-1}, \quad (8)$$

to $q_i + 1$ at higher energies, for which synchrotron-Compton losses dominate over the combined Coulomb and bremsstrahlung losses. To quantitatively compare the two distributions, and in order to assess the physical implications of using a PL form for the electron spectral density instead of the more realistic steady-state form, we first need to set the relative normalization. A physically meaningful way of doing so is by normalizing to the same energy density, $\rho = \rho_{pl}$,

$$\frac{k_i}{q_i - 1} \int_{\gamma_1}^{\gamma_2} \frac{\gamma^{-(q_i-2)} d\gamma}{b(\gamma)} = N_1 \int_{\gamma_1}^{\gamma_2} \gamma^{-(q_{pl}-1)} d\gamma. \quad (9)$$

Since the electron density is usually deduced from the synchrotron emission, a more observationally based choice is normalization to the measured radio flux. In the next section we compare results obtained based on these two different normalizations.

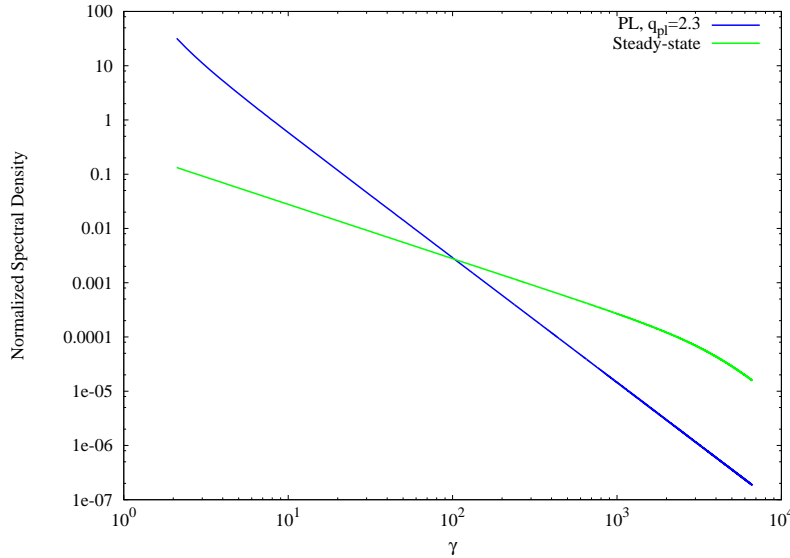


FIG. 1.— Electron steady-state and PL spectral densities for typical conditions in a SBN, normalized to the same energy density. Spectral densities were calculated with SBN parameters $q_{pl} = 2.3$, $q_i = 2.0$, $B = 100 \mu\text{G}$, $\rho \simeq 10 \text{ eV/cm}^{-3}$, $n_i = 200 \text{ cm}^{-3}$, $n_H = 30 \text{ cm}^{-3}$, and $n_{H2} = 150 \text{ cm}^{-3}$.

In our numerical estimates we take the theoretically motivated (and observationally supported) value of the injection PL index $q_i = 2$, and the observationally deduced value of q_{pl} . An estimate of the latter quantity is obtained from the

measured PL index of the radio spectrum, typically in the range 0.7 ± 0.05 in the central SB region (as in the nearby SBGs M82 & NGC253; for references to the radio measurements, see Rephaeli, Arieli, & Persic 2010, and Persic & Rephaeli 2014). Due to the significant (nonlinear) dependence of the electron energy density, ρ_e , on the spectral index, we adopt the lower (1σ) end of the measured radio index of 0.65, which corresponds to the fiducial value $q_{pl} = 2.3$. Doing so we (conservatively) underestimate the impact on estimation of ρ_e due to approximating a steady-state spectral density with a PL distribution. The PL and steady-state spectral densities are shown in Figure 1 for typical conditions in the dense and intense SBN environment, with $B = 100 \mu\text{G}$, a total radiation field energy density which is estimated to be about $10 \text{ eV}/\text{cm}^{-3}$ (e.g., Porter & Strong 2005), or $\rho \simeq 40\rho_0$, where $\rho_0 \simeq 4.2 \times 10^{-13} \text{ erg}/\text{cm}^{-3}$ is the (present value of the) CMB energy density. Assumed ionized and neutral gas densities are $n_i = 200 \text{ cm}^{-3}$, $n_H = 30 \text{ cm}^{-3}$, and $n_{H2} = 150 \text{ cm}^{-3}$.

The spectral densities plotted in Figure 1 clearly demonstrate that Coulomb losses dominate up to relatively high energies, $\sim 1 \text{ GeV}$ in a SBN. In fact, this is so not only in the high density, high magnetic field environment of a SBN, but also across the disk of star-forming galaxies for which both the gas density, $O(1) \text{ cm}^{-3}$, and magnetic field, $B < 10 \mu\text{G}$, are (correspondingly) lower than in a SBN, so that the ratio $n_i^{1/2}/B$ is roughly comparable to that in a SBN. However, the highest characteristic frequency ($\propto B$) at this critical value of γ is obviously much higher in a SBN than its typical value across the disk of a star-forming galaxy.

3. SYNCHROTRON AND COMPTON SPECTRA

The standard formula for the synchrotron emissivity by an isotropically distributed population of electrons with PL spectral density $N_1 \gamma^{-q_{pl}}$ is (Blumenthal & Gould 1970)

$$j_{pl}(\nu) = \frac{\sqrt{3}e^3 B N_1}{4\pi m c^2} \int \sin(\theta) d\Omega \int_{\gamma_1}^{\gamma_2} \gamma^{-q_{pl}} d\gamma \frac{\nu}{\nu_c} \int_{\nu/\nu_c}^{\infty} K_{5/3}(\xi) d\xi, \quad (10)$$

where e , m , c have their usual meaning, B is the mean magnetic field strength across the emitting region, θ is the pitch angle, $\nu_c = \nu_0 \gamma^2 \sin(\theta)$ is the characteristic synchrotron frequency, and $\nu_0 = 3eB/(4\pi mc)$ is the cyclotron frequency. The last integrand is the modified Bessel function of the 2nd kind, with an integral representation

$$K_{5/3}(\xi) = \int_0^{\infty} \exp^{-\xi \cosh(t)} \cosh(5t/3) dt. \quad (11)$$

It is usually assumed that for all frequencies of interest $\nu_c(\gamma_1) \ll \nu \ll \nu_c(\gamma_2)$, so that the γ integration can be well approximated by integration over the interval $[0, \infty]$. Doing so yields the standard formula

$$j_{pl}(\nu) = \frac{4\pi e^3}{m c^2} a(q_{pl}) N_1 B \left(\frac{\nu_0}{\nu} \right)^{(q_{pl}-1)/2}, \quad (12)$$

where $a(q_{pl})$ is expressed in terms of a ratio of Γ functions (eq. 4.60 of Blumenthal & Gould 1970).

For the steady-state electron density specified in eq. 7, the synchrotron emissivity is

$$j(\nu) = \frac{\sqrt{3}e^3 B k_i}{2m c^2 (q_i - 1)} \int_0^{\pi} \sin(\theta) d\theta \int_{\gamma_1}^{\gamma_2} \frac{\gamma^{-(q_i-1)}}{b(\gamma)} d\gamma \frac{\nu}{\nu_c} \int_{\nu/\nu_c}^{\infty} K_{5/3}(\xi) d\xi. \quad (13)$$

Using the above integral representation for $K_{5/3}(\xi)$, affecting the change of variable $x = \nu/[\nu_0 \gamma^2 \sin(\theta)]$, and extending the limits of the γ integration to $[0, \infty]$, we obtain the following 3D integral

$$j(\nu) = \frac{\sqrt{3}k_i}{4(q_i - 1)} \frac{e^3 B}{m c^2} \left(\frac{\nu_0}{\nu} \right)^{\frac{q_i}{2}} \int_0^{\pi} \sin(\theta)^{\frac{q_i+4}{2}} d\theta \int_0^{\infty} \frac{x^{q_i/2} dx}{b(\nu, \theta, x)} \int_0^{\infty} e^{-x \cosh(t)} \frac{\cosh(5t/3)}{\cosh(t)} dt, \quad (14)$$

where

$$b(\nu, \theta, x) = b_0(\nu_0/\nu) \sin(\theta) x + b_1[(\nu_0/\nu) \sin(\theta) x]^{1/2} + b_2. \quad (15)$$

(In a randomly oriented magnetic field the θ integral can be put in a closed form in terms of a combination of Whittaker functions [Crusius & Schlickeiser 1986].)

To compare the above curved steady-state spectrum to that of a PL distribution, we determine the spectral index that fits the most relevant range of the measured radio spectrum, and select a relation between the normalization factors N_1 and k_i . Given that energetic electron spectra are usually determined from radio emission, the relative normalization of the two distributions can be based on the measured flux at some characteristic frequency ν_c , $j_{pl}(\nu_c) = j(\nu_c)$. Below we compare results obtained with energy density normalization (specified in the previous section) to those obtained with the radio flux normalization.

Note that since the decay of charged pions (produced in proton-proton interactions) yields secondary electrons and positrons, which obviously contribute to the total synchrotron and Compton emission, the contributions of secondary electrons and positrons are essentially accounted for *approximately* by normalizing the electron spectral density to the measured (i.e., total emitted) radio flux. In our estimates of particle energy densities (in the next Section) this is quantified through the inclusion of the secondary-to-primary ratio, χ .

Since the most relevant range of the measured radio spectrum is $\sim 1 - 10$ GHz, and given that typically galactic radio spectra in the inner disk region are well fit by ~ 0.65 , the implied PL distribution is characterized by $q_{pl} = 2.3$. Of particular interest is the theoretically favored value $q_i = 2$, which for the most relevant frequency range is also in accord with a mean value of $\alpha \sim 0.65$. To assess the significance of employing the more realistic steady-state spectral distribution in the analysis of radio measurements, we consider the intense star-forming environment of a nuclear SB region in which the gas density and mean magnetic field are much higher than typical values across the galactic disk. We calculate $j_{pl}(\nu)$ with $q_{pl} = 2.3$, and $j(\nu)$ with $q_i = 2$, $B = 100 \mu\text{G}$, $n_i = 200 \text{ cm}^{-3}$, $n_H = 30 \text{ cm}^{-3}$, and $n_{H2} = 150 \text{ cm}^{-3}$, typical values in the nearby SBN of M82 & NGC253 (e.g., Persic & Rephaeli 2014). The spectra are shown in Figure 2 (in arbitrary units); the PL spectrum is shown for the case when the two distributions are normalized to the same flux at 5 GHz, and for the case when the distributions are normalized to the same energy density.

The different energy dependence of the loss processes results in a curved radio spectrum, with nearly a flat spectrum at very low frequencies to nearly a PL with an asymptotic index $q_i/2 = 1$ at high frequencies, corresponding to emission from high energy electrons whose losses are synchrotron-Compton dominated. As is evident from Figure 2, the overall impact of strong magnetic fields and high Coulomb losses on the synchrotron spectrum is a flattening that extends to relatively high frequencies well into the measured GHz range. Clearly, the synchrotron spectra shown in Figures 2 & 3 do not include the effect free-free absorption which decreases the emergent emission at very low frequencies (Condon 1982). Absorption is not included here primarily because our treatment is focused on the impact of spectral flattening due to electron energy losses, rather than on detailed modeling (and parameter extraction) in specific SBNs. In actual spectral fitting to the observed spectrum of a SBN, free-free absorption has to be modeled and accounted for before the spectral flattening due to particle losses can be determined, as was done by, e.g., Yoast-Hull et al. (2013, 2014a, 2014b).

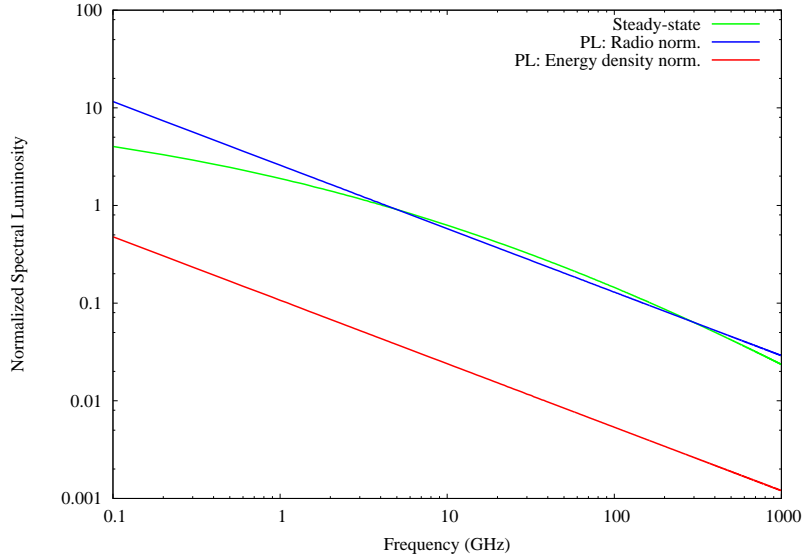


FIG. 2.— Normalized synchrotron spectra for steady-state and PL density distributions in a SBN region. The steady-state spectrum is shown by the green line; PL spectra are shown by the red and blue lines, with the relative normalization set to either the same energy density or to the same 5 GHz emissivity as that of the steady-state population, respectively. Spectral indices are $q_{pl} = 2.3$, and $q_i = 2.0$, and $B = 100 \mu\text{G}$.

Clearly, when the two distributions are normalized to the same energy density, the spectral emissivity of the PL is lower than that of the steady-state distribution. Since the steady-state spectrum was derived by explicitly accounting for electron losses at low energies, the spectral density can be extended down to the gas thermal energy, which is typically $O(1)$ keV. For our selected values of the PL index $q_{pl} = 2.3$ and source injection spectrum with index $q_i = 2$, the PL to steady-state energy density ratio reaches a value of 7.7 at kinetic energy of 511 keV ($\gamma_1 = 2$), and attains its maximal value 9.2 already at kinetic energies that are still much higher than the thermal gas energy ($kT \sim 1$ keV). The steeper the radio spectrum, the higher is the energy density ratio, which equals 17.4 and 33.6 for $\alpha = 0.7, 0.75$, i.e., for PL spectral densities with indices 2.4 and 2.5, respectively.

Since our treatment here is strictly spectral with no account taken of the spatial variation of the particle density across the galactic disk, extending the above description to the full disk is obviously unrealistic. However, our main objective here is to assess the impact of just replacing a PL distribution which, after all, is commonly assumed in characterizing particle spectra in galaxies, we carry out a similar calculation also for the full galactic disk. We realize, of course, that this is at best only a rough approximation of the more realistic description which necessarily involves a solution of a spectro-spatial kinetic equation. Repeating then the calculation with $B = 5 \mu\text{G}$, $n_i = 1 \text{ cm}^{-3}$, and $\rho = 4\rho_0$, which are typical mean values across the disk of a star-forming galaxy, and assuming a typical best-fit radio spectrum with $\alpha = 0.75$ (i.e., $q_{pl} = 2.5$), we obtain a value of 31.0 for the energy density ratio.

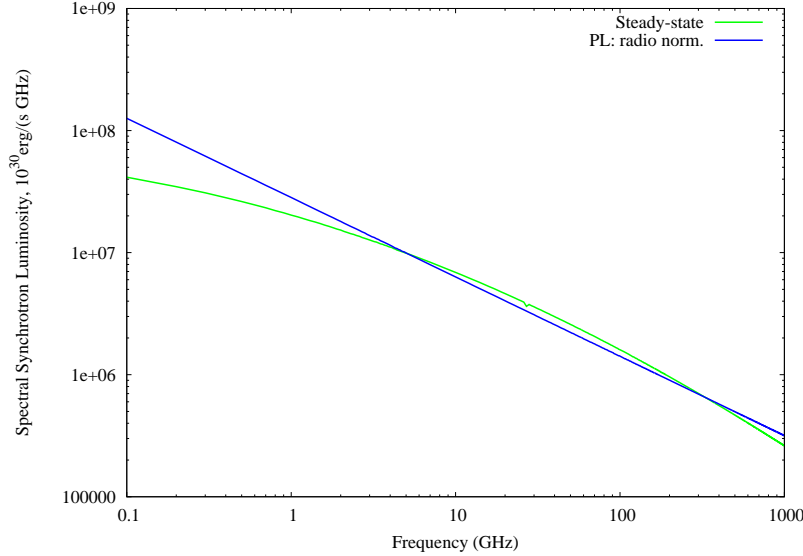


FIG. 3.— Synchrotron spectral luminosity from electrons with steady-state (green line) and PL (blue line) distributions in a SBN. The distributions were normalized to the same spectral luminosity at 5 GHz, $L_\nu \simeq 2 \times 10^{34}$ erg/(s Hz), with $q_{pl} = 2.3$, $q_i = 2.0$, and $B = 100 \mu\text{G}$.

The above large values of the energy density ratio reflect the fact that most of the energy density of the PL population is in lower energy electrons. Therefore, when the measured spectrum is fit by a PL, the density normalization is strongly weighted by the emissivity in the measured spectral range, and consequently the deduced energy density is much higher than that of the (curved) steady-state spectrum.

Normalizing the electron spectral density by the measured radio spectrum allows a direct prediction of the electron spectral Compton luminosity. Of particular interest is a comparison of the predicted X-ray and γ -ray spectral luminosity of a PL distribution in a SBN to that of a steady-state distribution. Integrations of the spectral Compton emissivity of an electron scattering off a diluted Planckian radiation field (in the Thomson limit; see, e.g., eq. 2.42 in Blumenthal & Gould 1970) over the electron PL and steady-state distributions, yield the spectra shown in Fig. 3. The distributions were normalized to the same spectral radio luminosity at 5 GHz, fiducially set to the measured flux from the SBN region of NGC253 at a distance of 3 Mpc.

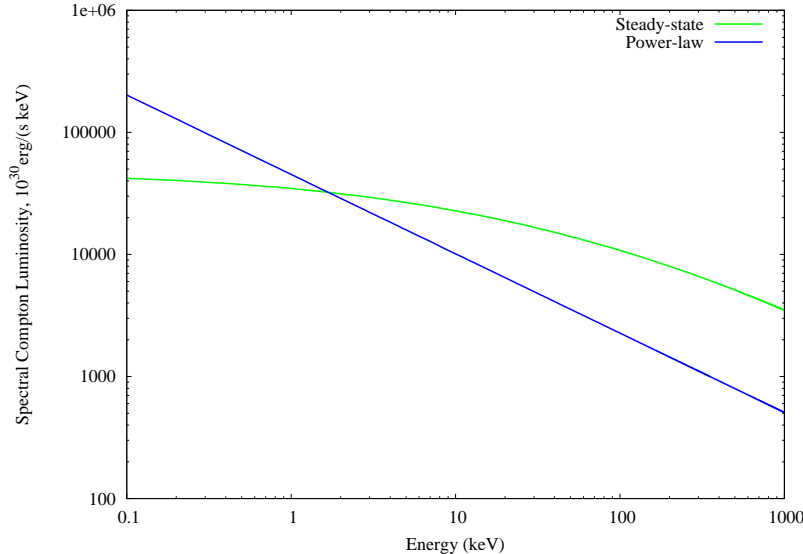


FIG. 4.— Compton spectral luminosity of electrons with steady-state (green line) and PL (blue line) distributions in a SBN. The distributions were normalized to the same spectral radio luminosity at 5 GHz, $L_\nu \simeq 2 \times 10^{34}$ erg/(s Hz), with $q_{pl} = 2.3$, $q_i = 2.0$, $B = 100 \mu\text{G}$, and diluted Planckian radiation field at a temperature $T = 40$ K and energy density $\rho = 40\rho_0$.

Comparison of the synchrotron and Compton spectra in Figures 3 & 4 demonstrates an important consequence of the observationally-based normalization of a steady-state electron distribution: The Compton yield of this distribution is significantly higher than that of the PL distribution that is normalized to the same radio flux. As is obvious from the latter figure, the spectral luminosity in the hard X-ray ($\epsilon > 10$ keV) and γ -ray is more than a factor ~ 5 higher

than that of the PL distribution. This is due to the fact that the electron spectrum is flatter at (a mean) energy $\epsilon = (4/3)\gamma^2\epsilon_0$, for which the Compton boost of the incident IR photon energy, ϵ_0 , yields an outgoing photon energy $\epsilon > 10$ keV.

4. PARTICLE AND MAGNETIC FIELD ENERGY DENSITIES FROM SYNCHROTRON EMISSION

In most cases of interest radio synchrotron measurements are analyzed for the purpose of determining energetic electron properties, such as density and energy density, and the mean strength of the magnetic field in the emitting region. As argued above, the common assumption of a PL distribution which is fit to the radio data can lead to very inaccurate values for these densities. Such estimates are also quite meaningless since in most cases the contribution of low energy particles is altogether ignored: For typical electron PL indices $2.3 - 2.5$, the fractional energy density at low energies (but still relativistic) below 1 GeV is $\sim 90\% - 97\%$, without even accounting for (sub-relativistic) supra-thermal electrons. Moreover, in many applications energy equipartition is assumed in order to determine the value of the mean magnetic field; for this purpose the proton energy density needs to be estimated. This is usually determined by adopting a theoretical relation for the proton-to-electron number density or energy density ratio. Therefore, overestimation of the electron energy density leads to overestimation also of the proton energy density and the field strength.

Quantifying the impact of the more realistic estimate of the electron energy density on estimates of the latter quantities necessitates a revised formulation of the common assumption of energy equipartition between energetic particles and magnetic fields: Since a state of equipartition is reached after a sufficiently long period of tight coupling between these nonthermal quantities, the asymptotic relation between their respective energy densities should be based on their steady-state distributions. Self-consistent calculation of these distributions (e.g., Rephaeli & Silk 1995, Lacki & Beck 2013) requires accounting for all energy loss processes of both electrons and protons, and for a description of the distributions across the full disk, also of their propagation modes. The quantitative description of such a more physically based equipartition state is outside the scope of our work here. As a first step towards this goal we describe here an approximate procedure that is based on the use (also) of a steady-state spectral density for the protons.

The relevant proton energy loss processes in ionized and neutral gas are Coulomb (i.e., electronic excitations and ionization), and pion production in proton-proton interactions. The respective loss rates, $b_{p,C}(\gamma)$ and $b_\pi(\gamma)$, can be expressed by the simplified formulae (adopted from Mannheim & Schlickeiser 1994)

$$b_C \simeq 3.32 \times 10^{-16} n_i \beta^2 \left[\frac{1}{\eta^3 + \beta^3} + \frac{1.2(n_{HI} + 2n_{H_2})}{n_i} \frac{(1 + 0.0185 \ln \beta)}{\beta_0^3 + 2\beta^3} \right] s^{-1}, \quad (16)$$

for $\beta \geq \beta_0 = 0.01$, and the temperature-dependent factor $\eta = 0.002(T/10^4\text{K})^{1/2}$. The loss rate due to pion production is

$$b_\pi \simeq 5.85 \times 10^{-16} n_i (\gamma - 1) \Theta(\gamma \geq \gamma_\pi) s^{-1} \quad (17)$$

where $\Theta(\gamma \geq \gamma_\pi)$ is a step function, and $\gamma_\pi = 2.3$ corresponds to the threshold kinetic energy for pion production, 1.22 GeV. At low energies electronic excitations is the only loss process, whereas at energies above 1.22 GeV losses are mostly due to pion production. An example for this spectral change is the drop in the local Galactic proton spectrum at low energies recently measured by the Voyager I spacecraft (Stone et al. 2013); as argued by Schlickeiser et al. (2014) this is due to Coulomb losses.

The proton injection spectrum is assumed to be PL in momentum which, when transformed to γ , can be written as $k_{p,i} \gamma(\gamma^2 - 1)^{-(q_{p,i}+1)/2}$.

$$\left(\frac{dN_p}{dt} \right)_i = k_{p,i} \gamma(\gamma^2 - 1)^{-(q_{p,i}+1)/2}, \quad (18)$$

which is valid also at low energies ($\gamma \simeq 1$). At steady-state the spectral density is simply

$$N_p(\gamma) = \frac{k_{p,i}(\gamma^2 - 1)^{-(q_{p,i}-1)/2}}{(q_{p,i} - 1)(b_C + b_\pi)}. \quad (19)$$

The resulting spectrum is $N_p(\gamma) \propto (\gamma^2 - 1)^{-(q_{p,i}-1)/2}$ at energies for which the loss rate is dominated by electronic excitations, steepening to $N_p(\gamma) \propto (\gamma - 1)^{-(q_{p,i}+1)/2}(\gamma + 1)^{-(q_{p,i}-1)/2}$ at energies (above 1.22 GeV) for which the loss rate is dominated by pion production.

The energetic proton density is usually related to that of the electrons by assuming a near equality in the rates energetic protons and electrons escape the acceleration region (e.g., Pohl 1993, Schlickeiser 2002). In the spirit of our approach here (whose objective is to estimate the impact of replacing a PL with a steady-state distribution), we adopt the charge neutrality assumption. In context of our approximate spectral (rather than spectro-spatial) steady-state treatment, the very different particle densities in the SBN and galactic disk would be explained as a consequence of the higher density of acceleration sites in the SBN, on the one hand, and the higher energy loss rates there on the other hand. If so, and equipartition is indeed attained, radio measurements then provide the observable needed to determine the proton energy density and mean strength of the magnetic field. Use of the more realistic particle steady-state distributions, and consideration of the full spectral range of particle energies, appreciably improve on the standard

calculation which is commonly based on PL spectra with a relatively high lower energy cutoff. Specifically, we extend our numerical example representative of conditions in the SBN of M82 and NGC253 (specified above) by computing also the proton energy density.

The proton source spectrum is a PL with nearly the same index as for the electrons, i.e. $q_{p,i} \simeq 2$, and the best-fit PL spectrum with index $q_{p,pl} = 2.2$, a value deduced from γ -ray measurements (Persic & Rephaeli 2014, and references therein). Repeating the calculations in the latter work (where all parameter values are specified) but with the steady-state spectra obtained here, we compute $\rho_p \simeq 75 \text{ eV cm}^{-3}$ and $B \simeq 56 \mu\text{G}$, as compared with $\sim 330 \text{ eV/cm}^{-3}$ and $\sim 120 \mu\text{G}$ when assuming PL spectral density distributions. Even though approximate, these values clearly show that the assumption of PL density spectra leads to significant overestimation of the electron energy density, and consequently also to overestimation of the proton and field energy densities (assuming equipartition).

5. DISCUSSION

The results presented in the previous section make it clear that the assumption of a PL distribution for energetic electrons and protons leads to large overestimation of their energy densities in comparison with the values deduced when more realistic steady-state spectral density distributions are used. We derived these distributions (self-consistently) by accounting for all relevant energy losses. Our quantitative estimates of the factors by which the electron energy densities are overestimated when deduced from radio measurements are in the range $\sim 10 - 30$ for radio spectral indices in the range $0.65 - 0.75$, when calculated for typical conditions in a SBN and the disk of a star-forming galaxy. The mere fact that in some of the analyses based on a PL distribution a high value of γ_1 is assumed (supposedly circumventing the need for explicit accounting for the spectral flattening due to Coulomb losses) does not reduce the inadequacy of the (single-index) PL model: Clearly, considerations of energy equipartition are not valid when the particle energy density is calculated over only part of the energy range, particularly so when the relatively large contribution of the lower energy particles is ignored.

Curved synchrotron spectra may also be a consequence of spatially inhomogeneous magnetic fields in the emitting region (e.g., Hardcastle 2013). Of course, particle spectra are intrinsically curved when the distribution is either time-varying (e.g., Torres et al. 2012) or before a steady-state is reached. In our treatment here (which is essentially complementary to the aforementioned works) we calculate self-consistently the synchrotron spectrum emitted by electrons whose spectral density is curved due to all the relevant energy losses sustained while traversing a region with a uniformly distributed gas, magnetic, and radiation fields. The impact of this more realistic modeling of the particle spectrum is usually more important than that of spatial variation of the gas density and magnetic field, especially for estimation of the particle total energy density in high-density environments (such as a SBN).

Compton scattering of relativistic electrons by IR and optical radiation fields in SBGs (Rephaeli, Gruber & Persic 1995, Wik et al. 2014a), and by the CMB in galaxy clusters (Rephaeli 1979, Wik et al. 2014b) is likely to contribute appreciably to their X-and- γ -ray spectra. As is clear from the spectra in Figure 4, estimating the level of hard X-ray emission by extrapolating the best-fit PL to the radio data can substantially under-predict the likelihood of its detection (and obviously affect motivation for its search). Moreover, the accuracy of joint analyses of radio and X-ray data can be improved substantially by using the properly normalized steady-state distribution for the electrons.

As specified in the previous section, low energy protons lose energy effectively by ionization (in neutral media) and energy excitation (in ionized gas), in addition to catastrophic losses in proton-proton interactions. Here we accounted for these energy losses under typical conditions in a SBN, as has been done for conditions in galaxy clusters (Rephaeli & Silk 1995) and SB galaxies (Lacki & Beck 2013). The effectiveness of Coulomb interactions of low energy electrons and protons with gaseous media obviously result in much lower steady-state spectral densities of low energy particles than what would be predicted from PL spectra. Overall, this implies that gas heating rates are correspondingly lower than estimated when assuming PL forms for the particle spectral density.

We are indebted to the referee for an expert and constructively critical review of the original version of this paper. The referee's suggestions and the changes made in their implementation considerably improved the paper. Work at UCSD was supported by a JCF grant. MP acknowledges the hospitality extended to him during a visit to UCSD.

REFERENCES

- Acciari, V.A., et al. (VERITAS Collaboration) 2009, *Nature*, 462, 770
- Acero, F., et al. (HESS Collaboration) 2009, *Science*, 326, 1080
- Ackermann, M., et al. (Fermi Collaboration) 2012, *ApJ*, 755, 164
- Blumenthal, G.R., & Gould, R.J. 1970, *Rev. Mod. Phys.*, 42, 237, *Rev. Mod. Phys.*, 42, 237
- Condon, J.J. 1982, *ARAA*, 30, 575
- Crusius, A., & Schlickeiser, R. 1986, *A&A*, 164, L16
- de Cea Del Pozo, E., Torres, D.F., & Rodriguez Marrero, A.Y. 2009, *ApJ*, 698, 1054
- Domingo-Santamaría, E., & Torres, D.F. 2005, *A&A*, 444, 403
- Gould, R.J. 1972, *Physica*, 60, 145
- Gould, R.J. 1975, *ApJ*, 196, 689
- Hardcastle, M.J. 2013, *MNRAS*, 433, 3364
- Lacki, B., & Beck, R. 2013, *MNRAS*, 430, 3171
- Mannheim, P., & Schlickeiser, R. 1994, *A&A*, 286, 983
- Persic, M., Rephaeli, Y., & Arieli, Y. 2008, *A&A*, 486, 143
- Persic, M., & Rephaeli, Y. 2010, *MNRAS*, 403, 1569
- Persic, M., & Rephaeli, Y. 2014, *A&A*, 567, A101
- Pohl, M. 1993, *A&A*, 270, 91
- Pohl, M. 1994, *A&A*, 287, 453
- Rephaeli, Y. 1979, *ApJ*, 227, 364
- Rephaeli, Y., Gruber, D.E., Persic, M. 1995, *A&A*, 300, 91
- Rephaeli, Y., & Silk, J. 1995 *ApJ*, 442, 91
- Rephaeli, Y., Arieli, Y., & Persic, M. 2010, *MNRAS*, 401, 473
- Rephaeli, Y., Nevalainen, J., Ohashi, T., & Bykov, A. 2008, *Space Science Reviews*, 134, 71
- Schlickeiser, R. 2002, *Cosmic Ray Astrophysics* (Berlin: Springer), p.472

- Schlickeiser, R., & Ruppel, J. 2010, New Journal of Physics 12, 033044
- Stone, E.C. et al. 2013, Science, 341, 6142
- Torres, D.F. 2004, ApJ, 617, 966
- Torres, D.F., Cillis, A., Lacki, B., & Rephaeli, Y. 2012, MNRAS, 423, 822
- Wik, D.R. et al. 2014a, ApJ, 792, 48
- Wik, D.R. et al. 2014b, arXiv:1411.1089
- Yeast-Hull, T.M. et al. 2013, ApJ 768, 53
- Yeast-Hull, T.M. et al. 2014a, ApJ 780, 137
- Yeast-Hull, T.M. et al. 2014b, ApJ 790, 86